Available online at www.sciencedirect.com

ScienceDirect

IFAC PapersOnline CONFERENCE PAPER ARCHIVE

IFAC PapersOnLine 55-32 (2022) 188–193

A hybrid dynamical systems approach to smart irrigation

R. Bertollo * **G.B. Cáceres** ** **P. Millán** ** **M. Pereira** ** **L. Zaccarian** *,***

* *Dipartimento di Ingegneria Industriale, University of Trento, Italy (e-mail: riccardo.bertollo@unitn.it)*

** *Universidad Loyola Andalucía, Dos Hermanas, Spain (email: gbcaceres@uloyola.es, pmillan@uloyola.es, mpereira@uloyola.es)*

*** *CNRS, LAAS, Université de Toulouse, France*

Abstract: We present a novel model for a drip irrigation system, using a hybrid dynamical systems paradigm to take into account the intrinsic binary nature of the control input. We consider an irrigation pipe with a generic number of drippers, analyzing the effect that the transients in the pipe have on the irrigation uniformity, and propose an intuitive irrigation strategy based on the one currently used by farmers. The model is presented together with simulations, whose parameters are based on real farm data.

1. INTRODUCTION

Irrigation is an essential agricultural practice where a certain amount of water is artificially applied to the soil, depending on the crop needs, see Oborkhale et al. (2015). In most farms, traditional surface water-saving systems are used, such us drip or sprinkler irrigation systems, because they save more water than alternative solutions, see Ohaba et al. (2012). In sprinkler irrigation, water escapes the pipes through rotating nozzles, with the goal of mimicking precipitations. This technique is useful to irrigate larger land areas due to its wider irrigation coverage (Evans and King (2010)). In drip irrigation, on the other hand, water is slowly supplied to the soil through small tubes near the crop roots, thus reducing the water loss caused by evaporation, which is influenced by wind and surface runoff, see Elasbah et al. (2019). Moreover, drip irrigation is typically more efficient, cheaper and requires less water flow to be operated.

According to Water (2018), in the agricultural sector, irrigation is responsible of 70% of the total water consumption. Additionally, in many countries, water availability is limited (De Fraiture and Wichelns (2010)), therefore policymakers around the world are creating strategies to achieve an efficient water usage (EC (2019a); EC (2019b)), and specialized agencies such as FAO (2022) promote the use of modern technologies to reduce the water consumption and, at the same time, increase the crop yield. Indeed, the classical irrigation strategy used by farmers consists in turning on the irrigation systems once or twice per day, with very long pulses, resulting in a good crop yield but a significant waste of water (Morillo et al. (2015)). A different irrigation strategy involving shorter pulses is difficult to propose without affecting the uniformity of the water distribution. This is mostly because of the effect of the sloping areas on the pipe water distribution uniformity (Ella et al. (2009)). Indeed, the transient associated with the pipe discharge process when irrigation is turned off, is known to generate uneven water distributions because of the gravity action. This phenomenon becomes more noticeable when the water distribution difference becomes comparable with the amount of water delivered during irrigation. Such non-uniformity in the crop yields is not desirable: this effect discourages an irrigation strategy based on shorter and more frequent water pulses, which on the other hand would significantly reduce the waste of water (Lozano et al. (2020)). For this reason, it is important to consider these transients when modelling an irrigation system and designing a realistic control strategy. Such novel approach is carried out here. Moreover, many of the proposed control strategies (Cáceres et al. (2021); Chen et al. (2021); Lozoya et al. (2014); Giusti and Marsili-Libelli (2015)), generate an optimal control input (namely, the water flow out of the emitters) that is persistently varying, and this is not practically feasible without significantly increasing the hardware cost. Indeed, without the use of expensive equipment, the only possible control on the system is to act on the valve that controls the water flow to the pipe, whose position is by definition binary (either open or closed).

In this work, we propose a novel model for a drip irrigation line, placed in a tunnel greenhouse. The model is characterized by three main features that make it a good representation of a real life scenario comprising: (1) the dynamics of the water in the soil, inspired from Cáceres et al. (2021), (2) the dynamics of the water in the pipe, (3) the binary nature of the control input. The representation of the valve position as a binary state is possible thanks to a hybrid dynamical systems formulation, combining continuous-time and discrete-time evolution in the following form Goebel et al. (2012)

$$\mathcal{H}: \begin{cases} \dot{x} = f(x), & x \in \mathcal{C}, \\ x^+ = g(x), & x \in \mathcal{D}, \end{cases} \tag{1}$$

where f, g are, respectively, the flow and jump map, and $\mathcal{C}$, $\mathcal{D}$ are the flow and jump set, where solutions may flow or jump, respectively.

The rest of this article is organized as follows: in Section 2 we recall the dynamics of the water in the soil, discussing some properties that allow for the practical implementation of our control algorithm; in Section 3 we present the dynamical equations for the water in the pipe and for the valve position, then we complete the hybrid formulation introducing an intuitive control strategy, which is inspired from the "practical" strategy used by farmers; lastly, in

10.1016/j.ifacol.2022.11.137

Section 4, we present some numerical simulations based on the parameters of a real farm, to show the behaviour of our model.

2. WATER DYNAMICS IN THE SOIL

2.1 Physical model and discretization

In order to describe the differential equations that characterize the water dynamics in the soil, according to Cáceres et al. (2021) and references therein, for each crop, the soil is divided into $N+1$ layers, as shown in the sketch at the right of Figure 1. The first layer is referred to as the surface layer, which is affected directly by precipitations and by the irrigation; the layers from 2 to N characterize the root zone, where the water is actually absorbed by the plant roots; the last layer $N+1$ is the drainage zone, used to keep track of the overflowing water, which should be minimized to avoid wasting resources.

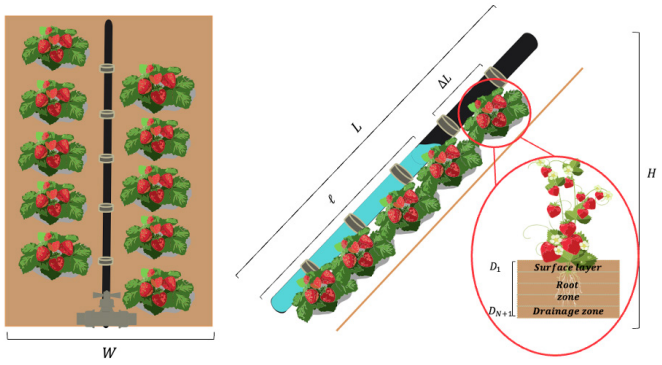

Fig. 1. Graphical representation of the irrigation line: view from above (left diagram), view from the side (middle diagram) and sketch of the soil layers (right diagram).

According to Cáceres et al. (2021), the dynamics of the soil moisture $\theta_i, i \in \{1,\dots,N+1\}$, for each layer, can be expressed though the following differential equations for each m^2 of field

$$\begin{aligned}
\dot\theta_1 &= f_1(\theta_1,\theta_2,u) := \frac{1}{D_1}\left(P(t) - Q_{1,2}(\theta_1,\theta_2) - E(t) + u\right)\\
\dot\theta_i &= f_i(\theta_{i-1},\theta_i,\theta_{i+1}) \qquad\qquad i \in \{2,\dots,N\}\\
&:= \frac{1}{D_i}\left(Q_{i-1,i}(\theta_{i-1},\theta_i) - Q_{i,i+1}(\theta_i,\theta_{i+1}) - E_{\text{root}}(t)\right)\\
\dot\theta_{N+1} &= f_{N+1}(\theta_N,\theta_{N+1})\\
&:= \frac{1}{D_{N+1}}\left(Q_{N,N+1}(\theta_N,\theta_{N+1}) - K_{N+1}(\theta_{N+1})\right),
\end{aligned} \tag{2}$$

where constant D_i is the thickness of the i-th layer, the input P represents the precipitations, the input E represents the water evaporation at the surface, E_{root} represents the water absorbed by the roots, u is the irrigation input, and the water flow $Q_{i,i+1}$ between consecutive soil layers is computed as

$$\begin{aligned}
Q_{i,i+1}(\theta_i,\theta_{i+1}) &:= \frac{B}{B+3}\left(\frac{1}{\overline{D}_i} + \frac{1}{\psi_{i+1}-\psi_i}\right)(H_i - H_{i+1}),\\
K_i(\theta_i) &:= K_{\text{sat}}\left(\frac{\theta_i}{\theta_{\text{sat}}}\right)^{2B+3},\\
\psi_i(\theta_i) &:= \psi_{\text{sat}}\left(\frac{\theta_i}{\theta_{\text{sat}}}\right)^{-B},\\
H_i(\theta_i) &:= K_i(\theta_i)\,\psi_i(\theta_i) = K_{\text{sat}}\psi_{\text{sat}}\left(\frac{\theta_i}{\theta_{\text{sat}}}\right)^{B+3},\\
\overline{D}_i &:= \frac{D_i + D_{i+1}}{2},
\end{aligned} \tag{3}$$

with constants $B, K_{\text{sat}}, \psi_{\text{sat}}, \theta_{\text{sat}}$ being empirical parameters depending on the soil composition. Note that, for compact notation, in the definition of $Q_{i,i+1}$ we sometimes removed the dependence on θ of H and ψ, which is highlighted in their respective definitions. Also note that, as we are considering irrigation in a greenhouse, in the simulations of Section 4 both the precipitations P and the surface evaporation E are set to zero.

To conclude, the dynamics in (2) can be written in a compact way as follows

$$\dot\Theta := \begin{bmatrix}\dot\theta_1\\ \dot\theta_2\\ \vdots\\ \dot\theta_{N+1}\end{bmatrix} = f(\Theta,u,t) := \begin{bmatrix}f_1(\theta_1,\theta_2,u,t)\\ f_2(\theta_1,\theta_2,\theta_3,t)\\ \vdots\\ f_{N+1}(\theta_N,\theta_{N+1})\end{bmatrix}, \tag{4}$$

where the dependence on t is through the external inputs P, E and E_{root}

2.2 Choice of the parameter N (monotonicity)

The model parameters to be selected are the layer thicknesses D_i, which are directly related to the number of layers N, since the soil depth is a given, constant value. A large number of layers N (or, which is the same, a small value of the layer thicknesses D_i) increases the accuracy of the model in approximating the original continuous version in Sellers et al. (1996). On the other hand, practical feasibility suffers from the choice of a high number of layers, which would require a higher number of sensors, to be placed at small distances; thus, a trade-off is needed.

An acceptable value of D_i in this sense can be selected as the maximum value such that the following assumption is satisfied.

Assumption 1. For all $i \in \{1,\dots,N\}$, D_i and D_{i+1} are chosen so that $\partial Q_{i,i+1}/\partial\theta_i > 0$ and $\partial Q_{i,i+1}/\partial\theta_{i+1} < 0$ for all the values in the considered soil moisture interval $[\theta_{\min},\theta_{\max}]$.

Remark 1. As we are dealing with an approximation of the theoretical model, it makes sense to select a portion of the state space where such an approximation needs to be accurate, as we did in Assumption 1. The lower limit $\theta_{\min}$ of the interval corresponds to the soil moisture at which the plant will die, while the upper limit $\theta_{\max}$ corresponds to the soil saturation limit for the specific case study, i.e. the maximum value of soil moisture before water starts overflowing. ○

Assumption 1 holds in the continuous version of the model Sellers et al. (1996), and such a requirement makes sense intuitively; indeed, we expect the water flow to increase when the soil moisture in the upper layer increases, and the converse to happen with the soil moisture in the lower layer.

To this end, we split the soil into equal layers (except for the first one, i.e. the surface layer) and we represent the surface $Q_{i,i+1}(\theta_i,\theta_{i+1})$, for increasing values of $D = D_i = D_{i+1}$. From the graphical analysis of the surfaces (see Figure 2 for some examples), we select the value $D = 3$cm, which satisfies Assumption 1.

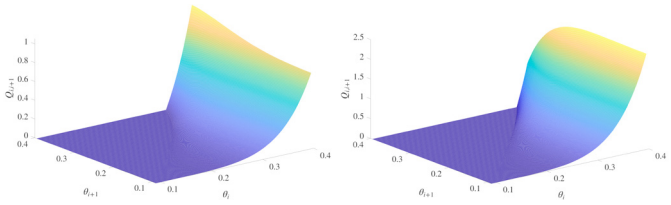

Fig. 2. Graphical representation of the water flow surface, for $D = 9$cm (left) and $D = 3$cm (right).

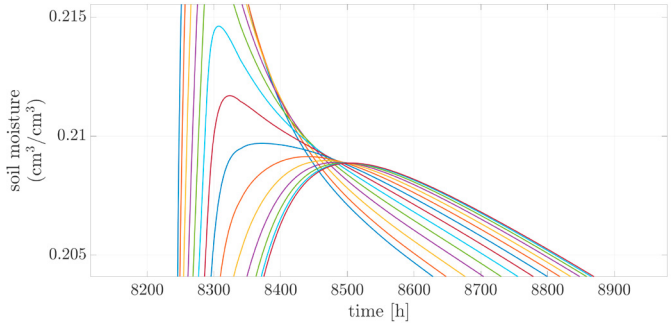

Fig. 3. Detail of the simulation in Section 4: the order of the soil moistures is not the same during the whole evolution of the system.

In view of Assumption 1, we can derive the following statements, whose proof is omitted due to space constraints.

Proposition 1. Under Assumption 1, each constant input $u(t, j) = \overline{u}$ corresponds to a unique equilibrium configuration $\Theta_{\text{eq}}(\overline{u}) = (\theta_{1,\text{eq}}(\overline{u}), \theta_{2,\text{eq}}(\overline{u}), \dots, \theta_{N+1,\text{eq}}(\overline{u}))$. Moreover, if $\overline{u}_2 \geq \overline{u}_1$ then $\theta_{i,\text{eq}}(\overline{u}_2) \geq \theta_{i,\text{eq}}(\overline{u}_1)$ for all $i \in \{1, \dots, N+1\}$.

Remark 2. Proposition 1 ensures that, if the crops along an irrigation line receive decreasing amounts of water, then the average soil moisture decreases too. This fact can be intuitively confirmed, observing that the crops at the top of an irrigation line are drier than the ones at the bottom. ∘

Remark 3. Selecting N sufficiently large, as suggested in this section, raises issues concerning the practical feasibility of the control scheme. Indeed, measuring all the states θ_i would require a significant increase in expenses. However, given the compartmental nature of this model, the soil moisture of the first and last layers of the root zone are reasonable upper and lower bounds for the soil moisture level of all the layers between them. This is confirmed by the simulations, see Section 4, and together with the monotonicity property shown in Proposition 1 it may allow us to use only two sensors for each irrigation line, which is reasonable.

Moreover, the monotonicity property along the irrigation line, shown in Proposition 1, suggests the possibility to exploit some similar monotonicity property across the layers in the soil. However, this property is disproven by simulations, as shown in Figure 3, depicting a zoomed portion of the simulation in Section 4, where we can see that the order of the soil moistures is reversed along the evolution of the system. This result highlights the need of different mathematical tools, and it will be investigated in future works. ∘

3. HYBRID DYNAMICAL MODEL

3.1 Water dynamics in the pipe

When we consider a set of M crops sequentially placed along an irrigation line, we must take into account the dynamics of the water in the pipe. In particular, we can assume a very fast filling, due to the high water pressure, while the emptying process is slower and non uniform, due to the difference in height among the crops along the same irrigation line (see the diagram in the middle of Figure 1).

According to these observations, we choose to model the pipe filling with an instantaneous change of the flow jumping to its steady-state value. Conversely, the pipe emptying can be modeled introducing a state representing the residual volume of water still contained in the pipe (or, which is the same up to rescaling, the length of the water column measured along the pipe axis ℓ). This value can be retrieved considering the whole pipe-crops system as a compartmental model, which gives

$$\ell(t) = L - \frac{\int_0^t \sum_j \mathcal{Q}_j(\tau) d\tau}{\pi r^2}, \tag{5}$$

where L is the length of the pipe, r is its radius, and $\mathcal{Q}_j$ is the volumetric flow out of the j-th dripper. The value of the flow $\mathcal{Q}_i$ out of a dripper as a function of the (relative) pressure p_i in the pipe can be modelled using the equation

$$\mathcal{Q}_j = k p_j^z,$$

where k is a constant given by the dripper type, and z is an empirical exponent whose value goes from about 0 (in the case of auto-compensated drippers) to 0.5 (in the case of non auto-compensated drippers).

Given the very slow discharge velocities in this application, we can consider the emptying process as a quasi-static phenomenon, therefore Bernoulli's principle gives

$$p_j = \rho_w g \max\{0, (\ell - \ell_j)\} \frac{H}{L},$$

where ρ_w is the water density, g is the gravity acceleration, ℓ_j is the position of the dripper, measured along the pipe axis, and H is the height difference between the starting and the ending point of the pipe. Combining the equations above, and differentiating (5), we obtain the dynamics of the state ℓ:

$$\begin{aligned} \dot{\ell} = f_\ell(\ell) &:= -\frac{\sum_j \mathcal{Q}_j}{\pi r^2} \\ &= -\frac{k}{\pi r^2} \left(\frac{\rho_w g H}{L} \right)^z \sum_j \left(\max\{0, (\ell - \ell_j)\} \right)^z . \end{aligned} \tag{6}$$

Summing up, the dynamics of the state ℓ depends on the valve position, and is represented by the following equations

$$\begin{aligned} &\dot{\ell} = f_\ell(\ell), && \text{with (OFF)}, \\ &\dot{\ell} = 0, && \text{with (ON)}, \\ &\ell^+ = L, && \text{with (OFF} \to \text{ON)}, \\ &\ell^+ = \ell, && \text{with (ON} \to \text{OFF)}. \end{aligned} \tag{7}$$

The (hybrid) dynamics in (7) can be written in a compact form by introducing a logic state q, representing the position of the valve. More precisely, we assign $q = 0$ when the valve is closed and $q = 1$ when it is open. Using this notation, we can rewrite (7) as

$$\begin{aligned} &\dot{\ell} = (1 - q) f_\ell(\ell), && \text{with (valve still)} \\ &\ell^+ = L, && \text{with (valve switch)}. \end{aligned}$$

Note that we simplified the jump map, since the pipe is always full while the valve is open, so in the ON-OFF transition we get $\ell^+ = \ell = L$.

Using the value of ℓ, we can also (algebraically) compute the value of the input $u_j(\ell)$ to the j-th crop, using the value of the volumetric flow $\mathcal{Q}_j$ out of the corresponding sprinkler. Since u is a linear flow in the vertical direction, averaged over a certain area, we must divide $\mathcal{Q}_j$ by the area $W\Delta L$ that each sprinkler is irrigating, where W is the tunnel width and ΔL is the distance between two consecutive sprinklers, measured along the pipe axis. This gives

$$u_j(\ell) = \frac{\mathcal{Q}_j}{W\Delta L} = \frac{k}{W\Delta L}\left(\frac{\rho_w g H}{L}\max\{0, \ell - \ell_j\}\right)^z. \quad (8)$$

3.2 Proposed control strategy

Since the control input is binary (valve open or closed), the control strategy corresponds to choosing the switching logic. From Proposition 1, it is clear that increasing the total amount of opening time of the valve results in a higher soil moisture. On the other hand, we know that frequent switching generates a non-uniform distribution of water among the crops due to the pipe depletion.

According to these facts, we propose here an intuitive control algorithm, consisting in a periodic switching (to be activated only at daytime, when the water absorption of the roots E_{root} is non-zero) regulated by two parameters, γ and ρ. In particular, the switching logic can be described using the following hybrid formulation

$$\begin{cases} \dot\tau_c = \rho, \\ \dot q = 0, \end{cases} \qquad \text{with } \tau_c \in [0,1],$$

$$\begin{cases} \tau_c^+ = 0, \\ q^+ = q, \end{cases} \qquad \text{with } \tau_c = 1, \quad (9)$$

$$\begin{cases} \tau_c^+ = \tau_c, \\ q^+ = 1 - q, \end{cases} \qquad \begin{array}{c}\text{with } (\tau_c \in [0,\gamma] \text{ and } q = 0) \\ \text{or } (\tau_c \in [\gamma, 1] \text{ and } q = 1)\,.\end{array}$$

In this hybrid dynamics, τ_c is a timer state that continuously evolves with derivative ρ and is reset to zero when its value reaches 1. The valve is opened when the value of the timer becomes larger than the threshold $1-\gamma$. Thus, practically speaking, $\rho > 0$ regulates the switching rate and consequently the irrigation uniformity, while $\gamma \in [0,1]$ regulates the average opening time, in a PWM fashion. Some examples of this hybrid dynamics are depicted in Figure 4, which clearly shows that a larger value of γ results in a larger percentage of time when the valve is open, whereas a larger value of ρ generates faster switching.

In view of the considerations above, the inputs γ and ρ can be selected based on some feedback quantity, in order to reach the desired distribution of soil moisture. Given the nature of this process, the (mean) effect of changes in γ and ρ on the soil moisture will take some time to be observed, thus the solution that we propose is to to keep γ and ρ constant during flows, and then periodically update them (in our simulations we perform updates every two days) according to some functions $g_\gamma(\Theta_1, \dots, \Theta_M), g_\rho(\Theta_1, \dots, \Theta_M)$, where Θ_j denotes the vector of the soil moistures at the j-th crop, as defined in (4).

A block diagram of the complete closed-loop system is depicted in Figure 5.

Remark 4. The proposed control algorithm is inspired by the irrigation strategy used by the farmers in a non automated context, i.e. providing pulses of water once or twice per day. While the final goal of a smart irrigation system is to optimize the pulse distribution in order to reduce the waste of resources, the feedback law proposed in this work only aims at showing the behaviour of the improved model of the irrigation line, without any claim of (9) being the optimal control strategy. The study of an improved control law will be the focus of future work. ∘

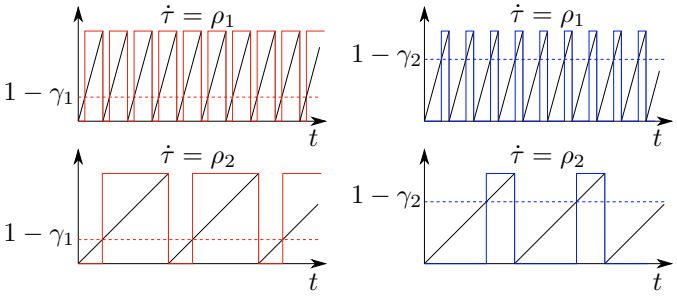

Fig. 4. Evolution of the timer τ_c (black, thin line), and the corresponding value of q (blue/red, heavy line) given by (9): $\gamma = \gamma_1 > \gamma_2$ (left plots) generates a signal with a larger mean value; $\rho = \rho_1 > \rho_2$ (upper plots) generates faster switching.

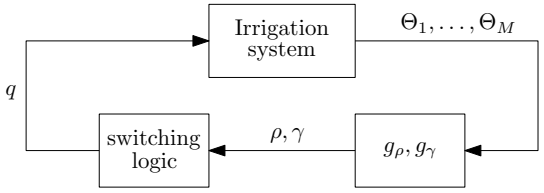

Fig. 5. Block diagram representation of the closed-loop system.

3.3 Complete hybrid model

The complete hybrid dynamics of the feedback system of Figure 5 is as follows. The flow dynamics stems directly from (4), (7), (8) and (9), and is given by

$$\dot x := \begin{bmatrix} \dot\Theta_1 \\ \vdots \\ \dot\Theta_M \\ \dot\ell \\ \dot q \\ \dot c \\ \dot\rho \\ \dot\gamma \\ \dot\tau_c \\ \dot\tau_{\text{day}} \\ \dot\tau_a \end{bmatrix} = f(x,t) := \begin{bmatrix} f(\Theta_1, u_1(\ell), t) \\ \vdots \\ f(\Theta_M, u_M(\ell), t) \\ (1-q)\, f_\ell(\ell) \\ 0 \\ 0 \\ 0 \\ 0 \\ c\rho \\ 1/60 \\ 1/60 \end{bmatrix}, \qquad x \in \mathcal{C}, \quad (10)$$

where the flow set $\mathcal{C}$ will be precisely characterized in the following, and we introduced three additional states $(c, \tau_{\text{day}}, \tau_a)$ to the description.

The timer states τ_{day} and τ_a in (10) keep track, respectively, of the hour of the day (in order to activate the control scheme) and of the elapsed time since the last adaptation of γ and ρ. The third state c is another logic state, which is set to 1 when the control algorithm is activated (i.e., at certain daytime hours), and to 0 when the controller is deactivated. Note that in (10) the flow map of τ_c contains this new state c, so that when $c = 0$

the control timer is frozen and the switching is deactivated, as desired.

Concerning the jump dynamics, we need to define different maps and sets to describe

(1) the valve switch
(2) the reset of τ_c when it reaches 1
(3) the reset of τ_{day} at the end of the day
(4) the adaptation of γ and ρ
(5) the control activation/deactivation

We now explicitly characterize each one of these maps $g_1(x), \dots, g_5(x)$, with the corresponding jump sets. Since they only affect some of the states, for compact notation we only report the jump dynamics of the affected states, while assuming that the other ones remain unchanged across the corresponding jump

$$\begin{bmatrix} l^+ \\ q^+ \end{bmatrix} = g_1(x) := \begin{bmatrix} L \\ 1-q \end{bmatrix}, \qquad x \in \mathcal{D}_1, \quad (11a)$$

$$[\tau_c^+] = g_2(x) := [0], \qquad x \in \mathcal{D}_2, \quad (11b)$$

$$[\tau_{\text{day}}^+] = g_3(x) := [0], \qquad x \in \mathcal{D}_3, \quad (11c)$$

$$\begin{bmatrix} \rho^+ \\ \gamma^+ \\ \tau_a^+ \end{bmatrix} = g_4(x) := \begin{bmatrix} g_\rho(\Theta_1, \dots, \Theta_M) \\ g_\gamma(\Theta_1, \dots, \Theta_M) \\ 0 \end{bmatrix}, \qquad x \in \mathcal{D}_4, \quad (11d)$$

$$\begin{bmatrix} c^+ \\ \tau_c^+ \end{bmatrix} = g_5(x) := \begin{bmatrix} 1-c \\ 0 \end{bmatrix}, \qquad x \in \mathcal{D}_5. \quad (11e)$$

The corresponding jump sets are given by

$$D_1 := \{x \in X : (\tau_c \le (1-\gamma) \text{ and } q = 1) \text{ or } (\tau_c \ge (1-\gamma) \text{ and } q = 0)\}, \quad (12a)$$

$$D_2 := \{x \in X : \tau_c = 1\}, \quad (12b)$$

$$D_3 := \{x \in X : \tau_{\text{day}} = 24\}, \quad (12c)$$

$$D_4 := \{x \in X : \tau_a = T_{\text{adapt}}\}, \quad (12d)$$

$$D_5 := \{x \in X : (\tau_{\text{day}} \in [h_{\text{ON}}, h_{\text{OFF}}] \text{ and } c = 0) \text{ or } (\tau_{\text{day}} \in [0, h_{\text{ON}}] \cup [h_{\text{OFF}}, 24] \text{ and } c = 1)\}. \quad (12e)$$

In (12), $h_{\text{ON}}, h_{\text{OFF}}$ and T_{adapt} are tuning parameters, corresponding to the hour of the day when the irrigation begins and ends, respectively, together with the amount of hours between two consecutive adaptations of γ and ρ. Lastly, the complete state space X is defined as

$$X := \mathbb{R}^{(N+1)M} \times [0, L] \times \{0, 1\}^2 \times \mathbb{R}_{>0} \times [0, 1]^2 \times [0, 24] \times [0, T_{\text{adapt}}]. \quad (13)$$

Using all the definitions in this section, we can characterize the hybrid system in the form (1), where the flow map f is defined in (10), the jump map is defined in terms of the graphs of the individual jump maps [1] in (11), namely

$$\text{gph } g(x) := \bigcup_{i \in \{1,\dots,5\}} \text{gph } g_i(x), \quad (14)$$

the flow set $\mathcal{C}$ is given by the closure of the complement of $\mathcal{D}$

$$\mathcal{C} := \overline{X \setminus \mathcal{D}}, \quad (15)$$

, and the jump set $\mathcal{D}$ is defined as the union of the jump sets in (12), namely

$$\mathcal{D} := \bigcup_{i \in \{1,\dots,5\}} \mathcal{D}_i. \quad (16)$$

[1] As the intersection among some of the jump sets in (12) is non-empty, strictly speaking the result of this operation would be a set-valued map, generating a hybrid inclusion. However, in view of the practical focus of this paper, we used this slight abuse of notation to avoid complicating the exposition.

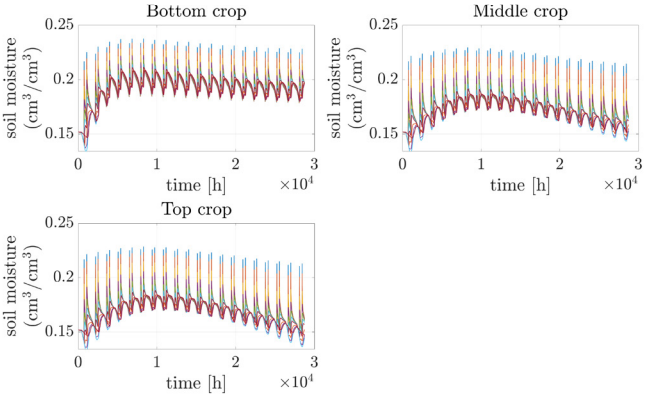

Fig. 6. Soil moisture evolution in the layers of three crops: bottom crop (top-left plot), middle crop (top-right plot) and upper crop (bottom-left plot).

4. SIMULATION RESULTS

In this section we present the results of simulations [2] performed on the proposed model. For our simulations, we selected the adaptation laws for γ and ρ to be

$$g_\gamma(\Theta_1, \dots, \Theta_M) := -k_\gamma \int_{t-\tau_a}^{t} (\Theta_{M,N}(\tau) - \mu) d\tau,$$

$$g_\rho(\Theta_1, \dots, \Theta_M) := -k_\rho \max\{0, \Gamma(t)\}$$

$$\Gamma(t) := \int_{t-\tau_a}^{t} \left(\frac{\Theta_{1,2}(\tau) + \Theta_{1,N}(\tau)}{2} - \frac{\Theta_{M,2}(\tau) + \Theta_{M,N}(\tau)}{2} - \sigma \right) d\tau,$$

where $\Theta_{j,i}$ represents the soil moisture θ_i of the j-th crop, μ is the desired average value for the soil moisture of the N-th layer of the highest crop, and σ is the tolerated mismatch between the average soil moistures of the first and last crop.

All the numerical values with the corresponding measurement units are reported in Table 1, with the exception of E_{root}, which is a time varying signal; the plot of its evolution during the day is not reported due to space constraints, but it can be retrieved from the typical values of the evapo-transpiration in this application, see for example (Cáceres et al., 2021, Figure 6), rescaling them according to the surface $W\Delta L$ considered here.

The simulation spans a period of 20 days, and the results are depicted in Figure 6, for some of the crops. In particular, we choose to report the evolution of the soil moisture for 3 crops, located respectively at the bottom, in the middle and at the top of the irrigation line. Even if the average value of the soil moisture of the last crop is not yet settled, we choose to show this portion of the simulation, to appreciate the spikes due to the irrigation in the single days.

From Figure 6, we can clearly see that the water distribution behaves as expected, and the lower crops in the irrigation line are characterized by larger average soil moisture. We can also observe that the initial values for γ, ρ cause a transient increase of the water content of the last crop above the desired value, but then the feedback (9) effectively reduces γ and consequently the average soil

[2] The simulations have been performed using the Matlab HyEQ toolbox Sanfelice et al. (2013)

Parameter	Value	Parameter	Value
D_1	1 cm	$D_{i,i\neq 1}$	3 cm
P	0	E	0
B	4.05	K_{sat}	1.056 cm/min
ψ_{sat}	12 cm	θ_{min}	0.09 cm^3/cm^3
$\theta_{\text{max}} = \theta_{\text{sat}}$	0.395 cm^3/cm^3	N	13
L	$5 \cdot 10^3$ cm	r	0.8 cm
k	$2.8 \cdot 10^{-4}$	z	0.5
ρ_w	0.997 g/cm^3	g	$3.53 \cdot 10^6$ cm/min^2
H	100 cm	ΔL	20 cm
W	60 cm	T_{adapt}	48
h_{ON}	7	h_{OFF}	20
k_ρ	$1 \cdot 10^{-5}$	μ	0.15 cm^3/cm^3
k_γ	$1 \cdot 10^{-4}$	σ	0.05 cm^3/cm^3

Variable	Initial condition	Value	Initial condition
$\Theta_{j,i,\text{init}}$	0.15 cm^3/cm^3	γ_{init}	0.13
ρ_{init}	$3 \cdot 10^{-3}$		

Table 1. Numerical values of the parameters and initial condition used in the simulation.

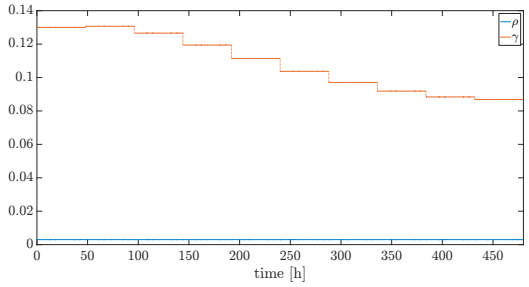

Fig. 7. Evolution of γ (red) and ρ (blue) during the simulation.

moisture, as we can see in Figure 7, where we depicted the evolution of ρ and γ.

5. CONCLUSIONS

In this work we proposed a novel model for irrigation lines with multiple crops and drippers. We used hybrid dynamical systems tools to model both the water dynamics in the pipe, when the latter is characterized by some slope, and the binary nature of the control input, corresponding to the valve position.

Taking inspiration from the non-automated irrigation strategy applied by farmers, we also proposed a preliminary hybrid feedback scheme, to stabilize the soil moisture close to a desired value, reducing the non-uniformity induced by the transients in the pipe. The behaviour of the model and the control scheme was illustrated through simulations, based on real farm data.

Future work will include a deeper analysis of the properties of this compartmental-like hybrid model, the design of an optimal control law and the analysis of the stability properties of the closed loop.

ACKNOWLEDGEMENTS

The authors thank the Spanish Agency for International Cooperation and Development (AECID) and the Junta de Andalucía, for partially funding this work, under projects Agricultura 4.0. (Grant 2020/ACDE/000192) and IRRIGATE (Grant PY20-RE-017-LOYOLA), respectively.

REFERENCES

Cáceres, G., Millán, P., Pereira, M., and Lozano, D. (2021). Smart farm irrigation: Model predictive control for economic optimal irrigation in agricolture. *Agronomy*, 11(9).

Chen, W.H., Shang, C., Zhu, S., Haldeman, K., Santiago, M., Stroock, A.D., and You, F. (2021). Data-driven robust model predictive control framework for stem water potential regulation and irrigation in water management. *Control Engineering Practice*, 113, 104841.

De Fraiture, C. and Wichelns, D. (2010). Satisfying future water demands for agriculture. *Agricultural water management*, 97(4), 502–511.

EC (2019a). European Commission: Farm to fork strategy. URL `https://ec.europa.eu/food/farm2fork_en`.

EC (2019b). European Commission: The European Green Deal. *COM/2019/640 final*.

Elasbah, R., Selim, T., Mirdan, A., and Berndtsson, R. (2019). Modeling of fertilizer transport for various fertigation scenarios under drip irrigation. *Water*, 11(5), 893.

Ella, V.B., Reyes, M.R., and Yoder, R. (2009). Effect of hydraulic head and slope on water distribution uniformity of a low-cost drip irrigation system. *Applied Engineering in Agriculture*, 25(3), 349–356.

Evans, R.G. and King, B.A. (2010). Site-specific sprinkler irrigation in a water limited future. In *Proceedings of the 5th National Decennial Irrigation Conference*, 1.

FAO (2022). URL `https://www.fao.org/home/es`.

Giusti, E. and Marsili-Libelli, S. (2015). A fuzzy decision support system for irrigation and water conservation in agriculture. *Env. Modelling & Software*, 63, 73–86.

Goebel, R., Sanfelice, R.G., and Teel, A.R. (2012). *Hybrid Dynamical Systems: Modeling, Stability, and Robustness*. Princeton University Press.

Lozano, D., Ruiz, N., Baeza, R., Contreras, J.I., and Gavilán, P. (2020). Effect of pulse drip irrigation duration on water distribution uniformity. *Water*, 12(8), 2276.

Lozoya, C., Mendoza, C., Mejía, L., Quintana, J., Mendoza, G., Bustillos, M., Arras, O., and Solís, L. (2014). Model predictive control for closed-loop irrigation. *IFAC Proceedings Volumes*, 47(3), 4429–4434.

Morillo, J.G., Díaz, J.A.R., Camacho, E., and Montesinos, P. (2015). Linking water footprint accounting with irrigation management in high value crops. *Journal of cleaner production*, 87, 594–602.

Oborkhale, L., Abioye, A., Egonwa, B., and Olalekan, T. (2015). Design and implementation of automatic irrigation control system. *IOSR Journal of Computer Engineering (IOSR-JCE)*, 17(4), 99–11.

Ohaba, M., Abidin, M., Li, Q., Shibusawa, S., Kodaira, M., and Osato, K. (2012). Adaptive control of capillary water flow under modified subsurface irrigation based on a SPAC model. In *Proc. of 11th International Conference on Precision Agriculture*.

Sanfelice, R., Copp, D., and Nanez, P. (2013). A toolbox for simulation of hybrid systems in matlab/simulink: Hybrid equations (hyeq) toolbox. In *Proceedings of the 16th International Conference on Hybrid Systems: Computation and Control*, 101–106.

Sellers, P., Randall, D., Collatz, G., Berry, J., Field, C., Dazlich, D., Zhang, C., Collelo, G., and Bounoua, L. (1996). A revised land surface parameterization (SiB2) for atmospheric GCMs. *Journal of Climate*, 9, 676–705.

Water, U. (2018). Nature-based solutions for water. *2018 UN World Water Development Report*.